Judging Method of Tooth Damage Behavior of the High Speed Milling Cutter

Minghui Zhang – Minli Zheng* – Bin Jiang

Harbin University of Science and Technology, National & Local United
Engineering Laboratory of High Efficiency Cutting and Tools, China

In the actual processing of the high speed milling cutter, due to the local damage of milling cutter components, the security and the decline in service life of the milling cutter generally exist, which seriously restricts its technical advantages of high-efficiency and high-precision processing. The tooth damage of the milling cutter is fuzzy and uncertain, which brings obstacles to the improvement of security stability and working efficiency of the milling cutter. The high speed milling cutter is subjected to high centrifugal force and cutting load during the milling process, resulting in damage to the milling components. Based on the material mechanical properties of milling cutter components and the impact experiment under a high strain rate, the damage types and formation mechanism of the milling cutter are analyzed, and the milling cutter damage model is established. The damage equivalent weight is adopted to quantitatively evaluate the damage degree of milling cutter teeth. Finite element simulation is used to find the vulnerable part of the milling cutter in high speed milling. Then the evolution process of milling cutter damage is analyzed, and the recognition and judgment method of milling cutter damage behavior is put forward, and lastly, this judgment method concerning the milling cutter damage is verified through experiment.
Keywords: high speed milling cutter, component material, strain rate, damage model

Highlights
• *Damage types and indexes were identified for the high speed milling cutter.*
• *A model that can calculate milling cutter damage under the centrifugal force, the dynamic cutting force and the pre-tightening force was established.*
• *The initial and the critical damage values were obtained by the cutting simulation and the high speed milling test.*
• *Damage behavior features of the milling cutter components materials were analyzed.*
• *A recognition and judgment method of milling cutter damage behavior was put forward.*

0 INTRODUCTION

With high efficiency, good quality and low energy consumption, the high speed milling technology represents the main development direction of the mold manufacturing [1] and [2]. In particular, the high speed milling cutter has been widely applied in the manufacturing field because of its superior performances and economic advantages [3]. Safety stability is not only the high-performance requirement of high speed milling cutter at a high level, but also the basis of the high speed and stable cutting. It not only fully demonstrates the safety state and performance of the milling cutter in the high speed cutting process, but also can comprehensively reflect the product economy and social satisfaction degree of the milling cutter [4]. It is the final criterion to examine whether the high speed milling cutter can meet the safety requirements of high efficiency and high precision machining of key components. Therefore, the damage mechanism of the high speed milling cutter is studied to prolong the safe and stable cutting time and improve milling efficiency and machining quality, which provides an important theoretical basis and engineering value for the design of more efficient and safer cutting tools,

and also plays a positive role in the development and application of the high speed milling technology.

At present, the guidance documents on the safety of high speed milling cutters all over the world mainly adopt the international standard ISO 15641 [5]. This method ensures the safe and stable operation of the high speed milling cutter, which is the prerequisite for high speed milling. However, this method can neither reveal the dynamic process of the decline in the safety of the high speed milling cutter, nor make clear the evolution process of the performance decline of the milling cutter caused by the damage of the milling cutter components such as the joint surface and screw.

The damage is the change of the local performance of the cutter body components caused by various external factors, which degrades the performance of the milling cutter. The cutter damage evolves from the micro defects in the material, and under the comprehensive action of the fatigue effect and the overload effect of the cutting load, when the micro damage accumulates to a certain extent, the vulnerable and unstable state may be broken at any time, and then massive macroscopic damage appears [6]. Li et al. [7] established an application research framework centering on in geometry, computer

*Corr. Author's Address: Harbin University of Science and Technology., Xuefu Road 52, Harbin, China, mh_zhang610@hotmail.com

simulation and finite element analysis based on the proposal of a small-to-large (micro structure - material structure - component structure) hierarchical multi-scale analysis method. Then the macro-mechanical response of the microstructure of the polycrystalline material was obtained, and the mechanical properties of the material were predicted. Cheng et al. [8] and Ge [9] proposed a microelement method suitable for the micro-macro scale-span analysis of new materials with the micro structure, which can realize the direct transition analysis from the material micro structure to the component macro response. Barabash et al. [10] studied the microstructural evolution of tool materials and revealed the inherent relationship between the geometric construction of the microstructure component, micro crack behavior and microstructure failure. Birck et al. [11] analyzed the characteristics in the damage process using the grid discrete element method. Jiang et al. [12] carried out the molecular dynamics simulation to simulate the mesoscopic state of the milling cutter and its components under different stress conditions using MAPS software. It was found that the sensitivity of the mesoscopic motion to external stress was different. Based on this, a quantitative analysis of the safety of the milling cutter was conducted, and then an evaluation model of milling tool efficiency life was established. In summary, the material damage of milling cutter components is imperceptible in the early formation stage, and it has more mesoscopic and microscopic characteristics.

Because the milling cutter has many design parameters, among which there are strong correlations, it is still difficult to fundamentally improve the tool structure form in order to improve the stability and cutting efficiency of the milling cutter. At present, it is more appropriate to optimize the corresponding parameters according to the specific functional requirements, and the goal is the form of driving,

which is the design concept of the milling cutter [13] and [14]. However, on the one hand, the optimization of parameters depends on empirical formulas and test data. On the other hand, there is a lack of scientific theories, and there are many ways to solve this problem at home and abroad, such as the parametric design method, TRIZ method [15], and axiomatic design method [16] and [17]. Although these methods play a certain guiding role in the decoupling of the milling cutter design technology, how to translate this abstract solution into a practical solution becomes the primary difficulty. In practical application, it is not fully developed, and it is still necessary to carry out further study.

The damage of the high speed milling cutter will lead to the changes in dynamic characteristics of the tool structure, which will be reflected by the different damage indexes of the milling cutter. By identifying the damage types, the state of the milling cutter before and after damage can be visually compared. Therefore, obtaining all kinds of damage indexes is the key factor to analyze the damage of the milling cutter. In this paper, a new physical quantity of equivalent damage is introduced, which directly reflects the damage evolution process in the system unit. By studying the relationship between various damages and the safety of milling cutters, an effective way to restrain the damage of high speed milling cutters is provided.

1 METHODOLOGY, OBJECTIVE, AND SCOPE OF THE RESEARCH

The performance of the high speed milling cutter mostly depends on several factors, such as, the materials composing the cutter components, the cutter structure, the selection of the insert coating and the rationality of the design [17]. Among them, the materials of the cutter components are its inherent attribute which is the precondition for studying the
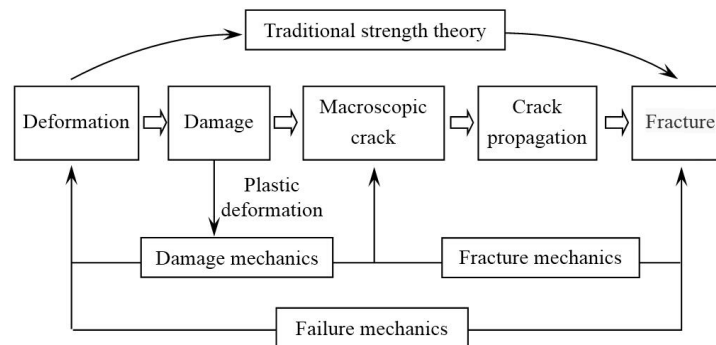

Fig. 1. Theory of damage analysis of milling cutter materials

damage of the milling cutter. The study on the damage mechanism of the high speed milling cutter is carried out on the basis of damage mechanics shown in Fig. 1. This paper studies the process of the deformation, development and destruction of the cutter materials along with the cutter when the cutter is subject to different external loads.

Starting from materials science, the macroscopic physical properties of the component materials of the high speed milling cutter are determined by its own atoms or molecules. The performance of the cutter can vary significantly depending on the properties of materials [18]. Therefore, the properties of the cutter components are very important for the cutting performance of the cutter. In fact, the damage has already been in existence in the manufacturing, production and processing of the material processing. The initial damage is inherent in the material itself, and the microcrack expansion rate is determined by the external load. As a result, the damage value depends on the material properties and the structural parameters of the cutter components. The various components of the high speed face milling cutter are not mutually independent. Instead, there is a connection structure. In addition, the functions of each component are different. Therefore, according to the actual role of the high speed milling cutter in

the cutting process, the functions of the milling cutter includes the connecting of the cutter bar to the milling cutter and the machine tool, the connecting of the screw to the insert, the connecting of the screw to the cutter body, the supporting of the milling cutter body and the cutting of the insert.

The high speed milling cutter is connected to the tool system in the cutting process. Thus, there is a constraint relationship between the cutter and the tool system. The principal axis direction is stipulated as Z-axis, the feed direction as X-axis and the line spacing direction as Y-axis. During the cutting process, the loading of the milling cutter mainly include the centrifugal force formed by the high-speed tool rotation, the pretightening force to tighten the screw and the cutting force imposed on the cutting edge. The forces are illustrated in Fig. 2.

In Fig. 2, F_z is the pre-tightening force imposed to the milling cutter mounting surface; P_e is the centrifugal force, n is the spindle speed, F_{ic} is the transient cutting force imposed to the cutting teeth, M_d is the running torque of the milling cutter, F_{id1} is the force imposed to the junction surface of the cutter body and insert side, F_{id2} is the force imposed to the junction of the cutting edge and the insert bottom, M_{i0} is the bending moment of the screw and F_{i0} is the force imposed to the junction of the screw and the insert.
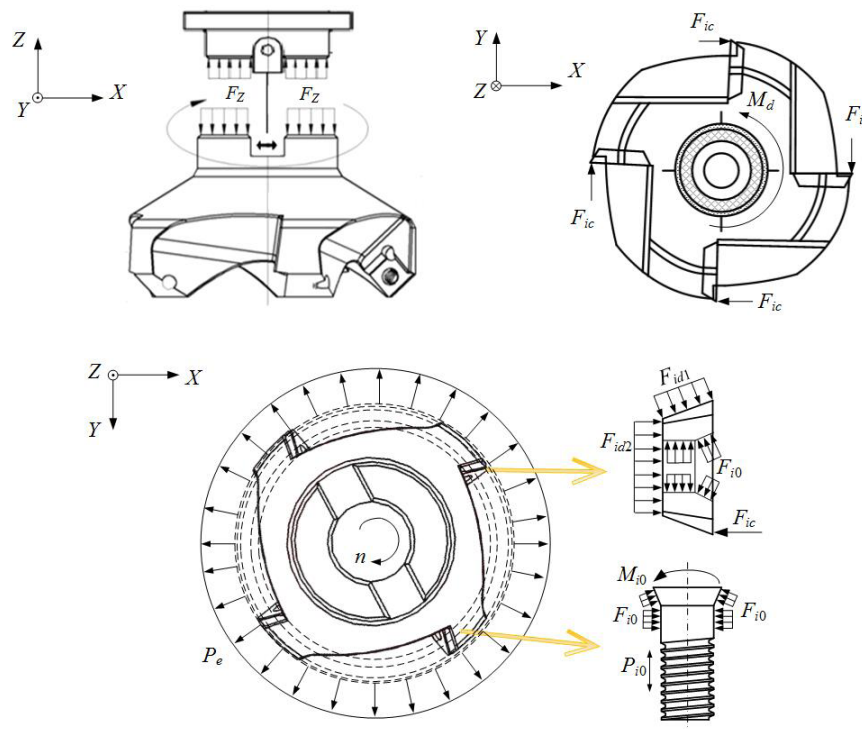

Fig. 2. *Force analysis in the cutting process of the milling cutter*

In high speed milling, the cutting force is directly imposed to the insert and is transmitted and distributed to the milling cutter components. The different loads of each component of the milling cutter lead to, the deformation of different properties of the locating surface of the cutter body and insert, and the joint surface of the insert and screw occurs, and the damage of different attributes can be further developed.

2 MODEL OF DAMAGE EVOLUTION OF THE MILLING CUTTER

In addition to the structure of the cutting tool, the critical damage value of the cutter components materials is the inherent nature of material itself. The equivalent volume element is adopted to establish the damage RVE model. It is assumed that the cutting tool material is isotropic, and the triaxial stress does not change over time. The initial defect expands from the microcrack and the initial damage of the RVE model starts to form.

The stress of the equivalent damage is adopted and the triaxial stress state is simplified to a uniaxial stress state unit model. The elastic strain energy density of the two models is the same. Considering the unilateral condition of crack closure, the equivalent damage stress can be expressed as:

$$\sigma^* = \sqrt{(1+\mu)\sigma^+ + \frac{1-D}{1-hD}\left((1+\mu)\sigma^- - \mu\sigma^2\right)}, \quad (1)$$

where σ^* is the equivalent damage stress; μ is the Poisson's ratio of the milling cutter component material; σ is the stress tensor of the triaxial state; D is the damage value of the milling cutter, and h is the microdefect closure parameter.

The initial damage value and the critical damage value are assumed to be the inherent properties of the milling cutter. For the selected milling cutter component, the microcrack propagation velocity is determined by the external load. The change of the RVE damage value of the milling cutter with the stress is shown in Fig. 3.

It can be seen from Fig. 3 that the damage value at the starting point of the curve is close to zero. It is believed that the damage value at this starting point is the initial damage value of the cutter materials. As the stress increases and exceeds a certain value, the damage value grows accordingly and then rises rapidly. The damage critical value depends on the material properties of the high speed milling cutter components and the deformation properties of the milling cutter. The damage value of RVE is determined by the material properties of the milling

cutter components and the structure parameters of the material. The analysis indicates that the overall trend of the milling cutter damage is that the value of equivalent damage grows with the increase of the stress.
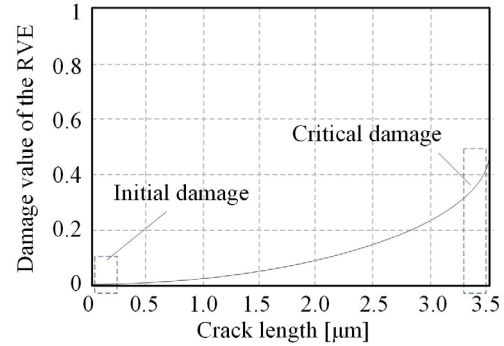

Fig. 3. *Model of damage of the milling cutter changing with stress*

A sliding crack model based on micromechanics theory is adopted to solve the problem of crack propagation under the compressive stress. A representative study of the crack performance under the compressive stress is the sliding crack morphology presented by Horii et al. [19], which is shown in Fig. 4. The curved microcrack is replaced by a straight line, and the open crack is generated at the tip of the microcrack. The axial compressive stress does not directly determine the expansion direction of the initial open crack, and there is a great angle between them. When the microcrack evolves into the medium term, the open crack will extend in the direction of the axial compressive stress. And when the open crack extends in the direction of the maximum axial compressive stress, its geometrical characteristics are obtained. The length of the initial microcrack is $2c$; the angle between the initial microcrack and the maximum axial compressive stress is θ, and the length of all the open cracks is l.

In a damage system, each micro void or microcrack is considered as a quasiparticle, whose evolution can be described in the damage state space. In the phase space, the state variable can be the dimension and orientation of the micropores or microcracks as well as the position coordinates of real space. Let $n(P_i, Q_i)$ be the number density of the microdamage. According to the law of conservation, the evolution of the damage can be expressed as:

$$\frac{\partial n}{\partial t} + \sum_i \frac{\partial (nP_i)}{\partial P_i} + \sum_i \frac{\partial (nQ_i)}{\partial Q_i} = n_N - n_A, \quad (2)$$

where n_A is the nucleation rate of the microdamage; n_N is the elimination coefficient caused by the convergence and healing of the microdamage; P_i is the damage evolution sensitivity; Q_i is the degree of insensitivity to damage evolution. The time rate can be taken as 0 and the nucleation rate before the damage critical period can also be viewed as 0. Eq. (2) can be rewritten as:

$$\frac{\partial n}{\partial t} + \sum_i \frac{\partial (nP_i)}{\partial P_i} = n_N. \qquad (3)$$
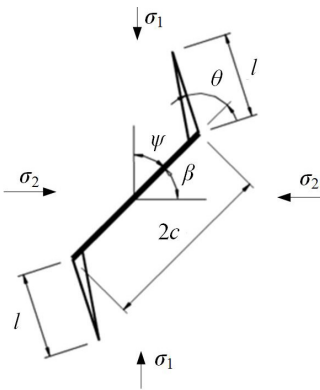
Fig. 4. *Sliding model of the microcrack*

The cyclic mechanical load in high-speed milling causes the accumulation of the milling cutter damage, which first appears at the micro meso level, eventually leading to the macroscopic fatigue crack propagation in the macro level of the tool materials. All these will produce damages. The initial defects existing in the high-speed milling cutter and its component material unit are mainly microcracks. It is assumed that these cracks are evenly distributed and interact with each other. Considering the interaction between microcracks, the sliding microcrack model including the sliding microcrack array under the stress state is established. The strains ε_1 and ε_2 caused by axial compressive stress σ_c can be expressed as:

$$(\varepsilon_1, \varepsilon_2)^T = (\varepsilon_1^e + \Delta\varepsilon_1, \varepsilon_2^e + \Delta\varepsilon_2)^T, \qquad (4)$$

where ε_1^e and ε_2^e are the elastic strains in the undamaged condition. $\Delta\varepsilon_1$ and $\Delta\varepsilon_2$ are the total loss strain caused by the initial microcrack slip and the sliding crack propagation. The elastic strain is shown in Eq. (5).

$$(\varepsilon_1^0, \varepsilon_2^0)^T = \frac{(\kappa+1)(\mu+1)}{4E} \begin{bmatrix} 1 & \dfrac{\kappa-3}{\kappa+1} \\ \dfrac{\kappa-3}{\kappa+1} & 1 \end{bmatrix} (\sigma_c, 0)^T, \quad (5)$$

where E is the elasticity modulus of the cutter material and μ is the Poisson's ratio of the cutter material.

$$\begin{cases} \kappa = 3 - 4\mu & \text{(plane strain)} \\ \kappa = [(3-\mu)(1+\mu)] & \text{(plane stress)} \end{cases}. \qquad (6)$$

Since the current problem is a linear one, it can be considered that the damage strain is relevant to the fact that the externally loaded axial stress σ_c is linear. It is assumed that there are N initial microcrack defects in the cutter material unit model. The interaction between the micro cracks is not considered. Then, the total damage strain of the tool material unit can be written as:

$$(\varepsilon_1, \varepsilon_2)^T = \left((\varepsilon_1^0, \varepsilon_2^0)^T + N \begin{bmatrix} S_{11} & S_{12} \\ S_{21} & S_{22} \end{bmatrix} \right) (\sigma_c, 0)^T, \quad (7)$$

when $\varepsilon_1 = \varepsilon_2$, there is:

$$\sigma_c = \frac{E\varepsilon}{1 + ENS_{11}}. \qquad (8)$$

It can be seen that under the effect of axial compressive stress, the strain of the material is controlled by the elasticity modulus, and the elastic modulus at this time is smaller than that in the case of damage accumulation. E_D is adopted to define the material unit damage. Then, Eq. (8) can be simplified as:

$$\sigma_c = E_D\varepsilon = E(1-D)\varepsilon. \qquad (9)$$

Therefore, the damage of the milling cutter component unit can be obtained through solving Eq. (8) and (9) simultaneously. The equation is as follows:

$$D = 1 - \frac{E}{1 + ENS_{11}}. \qquad (10)$$

The effective stress in the damage state can be obtained by applying the equivalent damage value D and the equivalent damage stress conducive to analyzing the mechanism of the milling cutter damage.

3 RESULTS

3.1 Cutting Tool Materials

This paper analyzes the milling cutter damage formation and evolution process taking the indexable four-tooth high speed face milling cutter with a diameter of 63 mm and equal teeth distance as an example. Its tool cutting edge angle is 45°, flank angle is 20°, rake angle is 0°, and edge inclination angle is 10°. The shape of the milling cutter is shown in Fig.

5. The cutter components include the cutter body, the corresponding materials of the screw and the cutting edge materials. The mass fractions of the elements in the materials are listed in Tables 1 and 2.
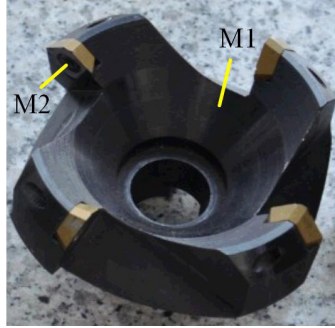

Fig. 5. *Four-tooth high speed face milling cutter with a diameter of 63 mm*

Table 1. *Chemical composition of the materials in the milling cutter body and screw*

Components	C	Si	Mn	Cr	Ni	P	S
M1	0.45	0.27	0.73	1.10	0.27	0.03	0.03
M2	0.39	0.21	0.64	1.08	0.15	0.03	0.02

Table 2. *Chemical composition of the materials in the milling cutting edge*

Component	W	C	Co	O
Insert	68.67	21.77	7.54	2.02

3.2 Damage Behavior Features of the Milling Cutter Components

The tensile and compression tests of the cutter component materials were carried out on a WDW-200 computer control electronic universal testing machine under the same load level and the stress-strain curves are shown in Fig. 6. The shape of the stress-strain curve in Fig. 6 reflects the various deformation processes of the materials, including the elastic deformation stage, the plastic deformation stage, the necking deformation stage and the strengthening stage under the action of external load.

The traditional material mechanics strength theory has limitations. It is learned from ordinary physics that atoms interact with each other: when the atomic spacing is small, they repel each other; when the spacing is large, they attract each other. The cutter materials are damaged when the binding force between atoms are overcome. The distance increases with the growth of the stress value. When the stress overcomes the binding force between atoms and reaches the maximum value σ_m of the action force, this value is the theoretical fracture strength.

However, numerous test results and engineering applications indicats that the actual fracture strength of the material is one to three orders of magnitude smaller than the theoretical fracture strength, which is because there must be various defects in the actual materials, such as microscopic cracks, vacancies, incisions, and scores, to decline the safety and stability of the tool and reduce the tool life. For the real milling cutter component materials, the ductile fracture process under tensile stress is the process of pulling the atoms apart along the direction which is vertical to the tensile stress. The approximate calculation formula of the microcrack intensity σ_t of the material can be approximated as:

$$\sigma_t = \left(K_m / \sqrt{2\pi} \right) \cdot \left(1/\sqrt{r_{ij}} \right) \cdot \tilde{\sigma}_{ij}, \qquad (11)$$

where K_m reflects the intensity level of the stress field near the tip of the insert cutting zone, ij reflects the second order tensor and r_{ij} reflects the second order tensor of the crack area. This formula stands for the stress solution in the crack area of the tool.

According to the stereoscan photograph of the test sample, which is shown in Fig. 7, the tensile fracture of each component of the milling cutter all presents as microporous aggregation fracture. Due to the intense slippage and the dislocation pileup, many micro voids are frequently seen in local area, or there
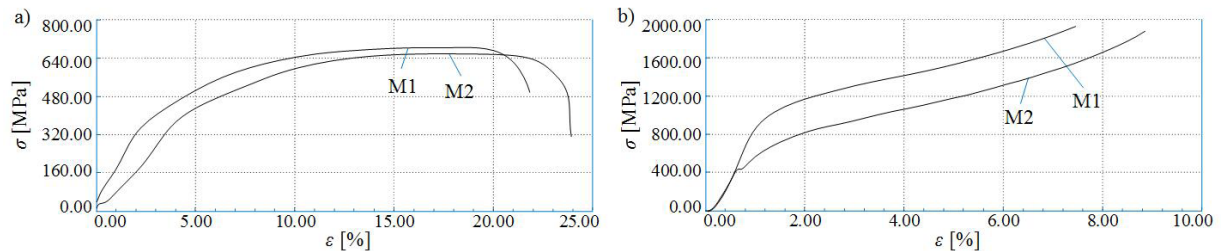

Fig. 6. *Formation and evolution of component material damage; a) tensile failure damage; and b) compression damage*
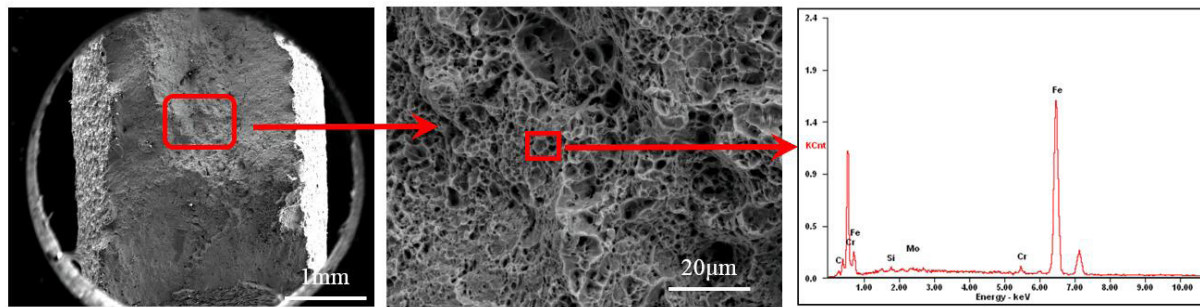
Fig. 7. *Scanning electron microscope observation and energy spectrum analysis*

are some impurities crushing, and fractures of foreign matters and base metal interface.

Fig. 7 shows that the fracture is not smooth, for the direction of crack propagation in the metal materials is relevant to the direction of maximum stress, and the crack propagation follows the path with the least resistance. The morphology and structure of the fracture directly record the occurrence of the fracture microcracks, the process of crack propagation and the ultimate moment of fracture. The fracture process of the tested materials develops from the local to the whole, including two processes: crack generation and crack propagation.

The mechanical responses of materials under different load conditions are quite different. Because the milling cutter is used for periodic intermittent cutting, the dynamic response under the impact load is needed. The stress-strain curve and strain rate were obtained by carrying out the impulse test to the milling cutter screw and cutter body materials under the impulsive pressures of 0.4 MPa, 0.6 MPa and 0.8 MPa using SHPB equipment. The stress-strain curves fitted by the stress-strain data collected using the data acquisition unit are shown in Figs. 8 and 9.

The transient waveform memory recorded the incident wave signal ε_i, reflected wave signal ε_r and
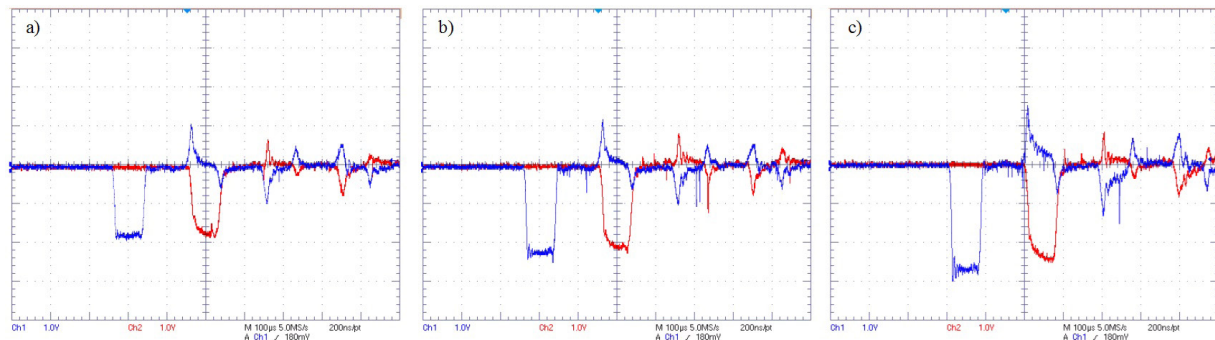

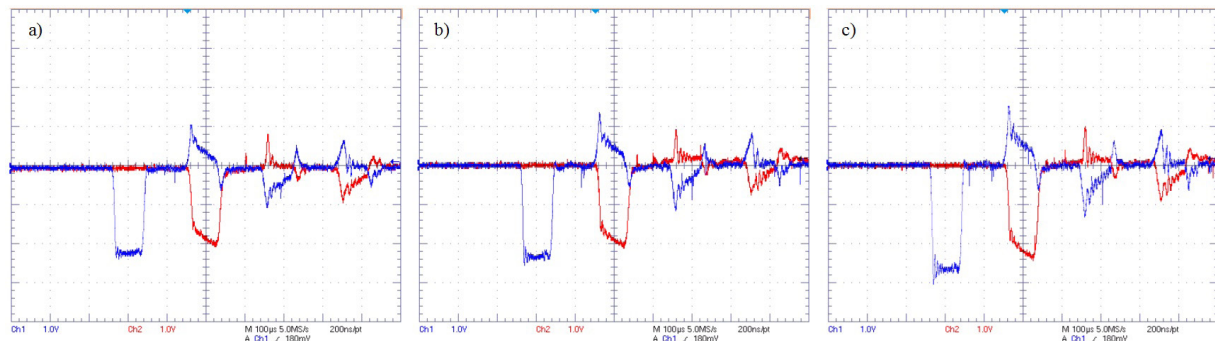**Fig. 8.** *M1 waveform of the milling cutter components under the impact; a) 0.4 MPa; b) 0.6 MPa; and c) 0.8 MPa*

Fig. 9. *M2 waveform of the milling cutter components under the impact; a) 0.4 MPa; b) 0.6 MPa; and c) 0.8 MPa*

the transmitted wave signal ε_t. Based on the theory of stress wave, the three signals, ε_i, ε_r and ε_t confirm the stress-strain relationship of the material, as shown in Eq. (12).

$$\varepsilon_s = -\frac{2c_0}{l_0} \int_0^l \varepsilon_r \cdot dt, \tag{12}$$

where ε_s is the average strain; c_0 refers to the wave velocity of the one-dimensional stress wave propagation in the rod; l_0 is the initial length of the test piece; ε_r is the strain of the reflected wave.

The average stress in the test is:

$$\bar{\sigma} = E \cdot A \cdot \varepsilon_t / A_s, \tag{13}$$

where E is the elasticity modulus of the incident bar; A is the sectional area of the incident bar; A_s is the sectional area of the specimen.

The stress and strain data of M1 and M2 materials of the milling cutter components under the load condition are fitted to curves, which are shown in Fig. 10.

The impact surface of the tested specimen under the impact effect was observed under the scanning microscope. It is discovered that the defects of the material after the impact are more obvious. Excluding the defects of the materials, the surface of the tested specimen under the impact load presents as a wavy interface, which is the basic organizational characteristics after the impact is imposed. It can be seen from the stress-strain curves of the above materials that with the increase of the stress, the yield limit of the material began to be linear and when it reaches a certain value, the yield capacity weakens dramatically, and the deformation extent starts to intensify.

Under the various stress levels, the strain rates of the milling cutter components at a variety of impact

levels are 231.0, 345.9, 891.5, 952.1, 1121.2, and 1311.9, respectively. It can be seen that the strain rates of the screw materials are lower than those of the cutter body materials, indicating that the screw materials have a poor capacity to withstand the load, while the cutter body materials have strong impact resistance ability.

The constitutive relation model of the milling cutter materials can be obtained using the Johnson-Cook (JC) model [20]. This model is suitable for a variety of conditions and can be used to describe the relationship between one function and its effect. Its basic form is as follows:

$$\sigma = [A + B(\bar{\varepsilon})^n] \left[1 + C \ln \left(\frac{\dot{\varepsilon}}{\dot{\varepsilon}_0} \right) \right] \left[1 - \left(\frac{T_\alpha - T_r}{T_m - T_r} \right)^m \right], \tag{14}$$

where A, B, C and m are constants; σ is the flow stress under nonzero strain rate; n is the work hardening index; $\bar{\varepsilon}$ is the equivalent plastic strain; $\dot{\varepsilon}$ is the equivalent plastic strain rate; $\dot{\varepsilon}_0$ is the reference strain rate, T_α is the test temperature, T_r is the reference temperature, T_m is the melting temperature.

After conversion and parameter fitting, the parameters of the JC model of the component materials of the milling cutter were obtained, as shown in Table 3.

Table 3. *Parameters of the JC model of the milling cutter components*

JC model variable	A [MPa]	B [MPa]	C	m	n
M1	20.516	61.367	0.0087	1.134	0.704
M2	19.452	57.423	0.0382	1.732	0.536

The strength of the material is the function of strain, strain rate and temperature. This model can be
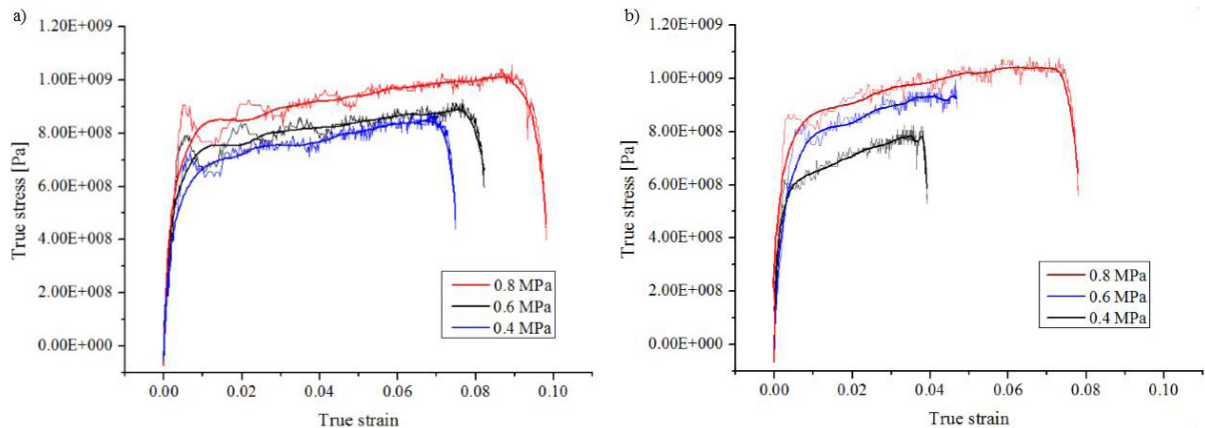

Fig. 10. *Strain-stress fitting curve of the milling cutter components; a) milling cutter material M1; and b) milling cutter material M2*

used to analyze the performance of the milling cutter materials and provide basis for studying the material conditions required in the various damages of the milling cutter.

The mechanical property of the component materials of the high speed milling cutter under a high strain rate and the stress-strain relationships of the component materials within the range of a high strain rate were obtained through the static load and impact experiment. These changing characteristics of the yield strength of component materials under different impact loads were analyzed and the rate of response of the materials to the external stress was obtained. All these provide experimental analysis basis to the milling cutter to resist the dynamic cutting force in the cutting process, thereby providing support to suppress the milling cutter damage and ensure efficient, stable and secure cutting.

3.3 Formation and Evolution of Milling Cutter Damage

According to the load analysis of the milling cutter components in the previous parts of this paper, the milling cutter is subject to multiple forces in the cutting process, including the centrifugal force, the dynamic cutting force and the prestressing force. Meanwhile, the surface-to-surface contact is formed between the upper end face of the tool and the knife handle. Under the action of the axial force, the cutter handle wedge determines the horizontal direction of the cutter handle end surface which is vertical to the upper end surface of the cutting miller. Besides, the horizontal displacement of this end surface is restricted. The high speed cutting experiment related to the cutting parameters in Table 4 is carried out by adopting the high speed milling cutter structure and

component materials listed in Part 3.1. The screw specification is M5.0, the locking torque is 5 Nm, and therefore the pretightening force of the milling cutter screw is 5.33 kN.

Table 4. *High speed milling test scheme*

Cutting speed v [m/min]	Milling depth a_p [mm]	Feed per tooth f [mm/r]	Milling width a_e [mm]
2000	0.5	0.08	56

Fig. 11 presents the loads and constraints imposed on the cutter in the finite element simulation.

Under the action of the centrifugal force, the dynamic cutting force and the pre-tightening force, the milling cutter is prone to suffer damage in such areas as the junction surface of the insert and the cutter body, the junction surface of the insert and the screw, the junction surface of the cutter body and the screw and the root of the cutter body and the cutter tooth. Next, these four areas will be analyzed.
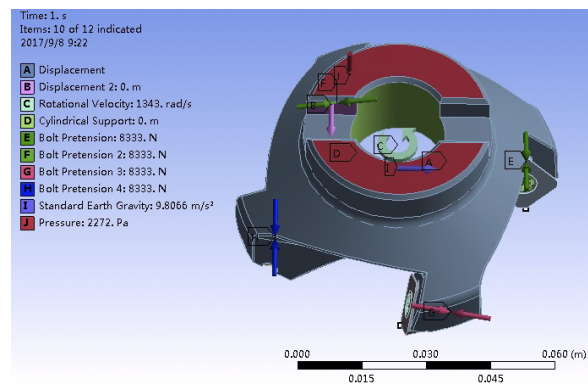

Fig. 11. *Load and constraint conditions imposed in the finite element*
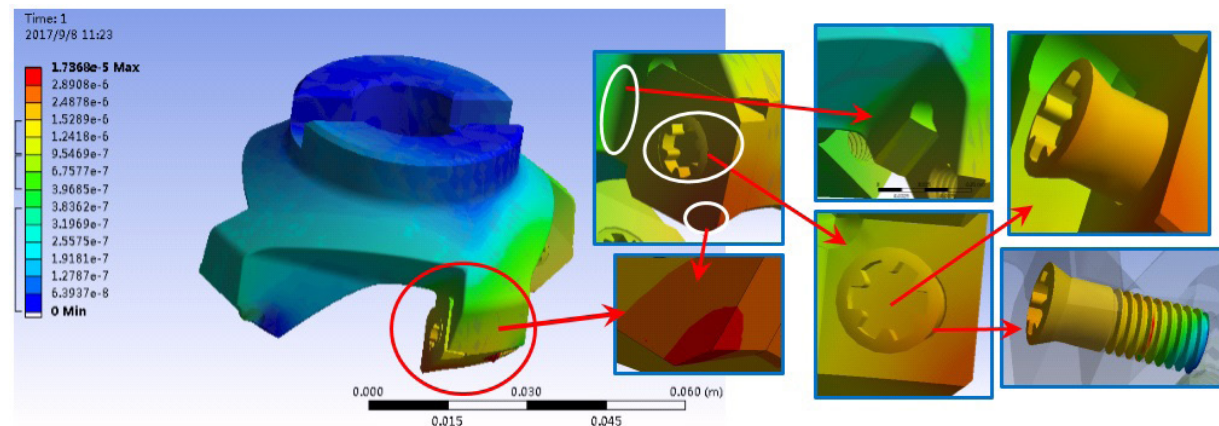

Fig. 12. *Division of the deformation zone of the milling cutter*

The deformation process of the screw head and the screw thread in high speed milling is explored, as shown in Fig. 13. It is demonstrated that the elastic deformation occurs in the screw head and the screw thread at the beginning of the process. With the continuous processing, the elastic deformation differs from the plastic deformation.
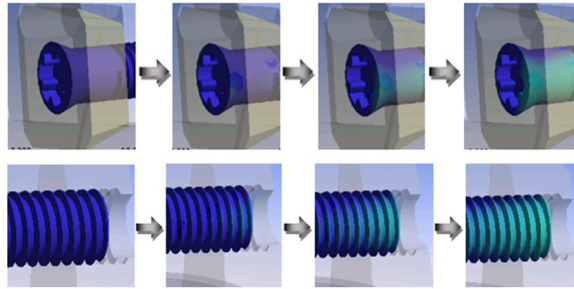

Fig. 13. *Formation and evolution of screw damage*

In this paper, the deformation process of the junction surface of the cutter body and insert in high speed milling is examined, as shown in Fig. 14. It is demonstrated that the compression deformations occur in joint surfaces. As the cutting force acts on the tool tip, the compression deformation in the tool tip is larger.
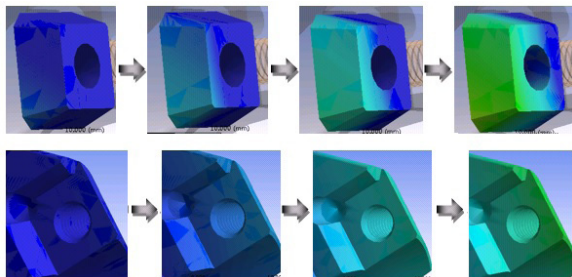

Fig. 14. *Formation and evolution of the damage to the joint surface of the insert and the cutter body*

As can be seen from the simulation analysis, the bolt pre-tightening force of the milling cutter components mainly have an impact on the locating surface of the insert and screw. The greater the pre-tightening force is, the greater the squeezing stress between the insert and the cutter body is, and the more obvious the compression deformation is. The pre-tightening force of the screw exerts an effect on mainly two parts of the insert: one is the locating surface between the insert and the cutter body, and the other is the locating surface between the insert and the screw. From the perspective of stress value, the impact of the pre-tightening force on the cutter components is not as obvious as that of the cutting force. Compression

damage occurs in the joint surface of the insert and the cutter body due to the impact of the cutting force. The action direction of the pre-tightening force is consistent with that of the main cutting force, which will intensify the degree of compressive injury of the joint surface.

3.4 Cutting Conditions

The high speed milling aluminum alloy 7075 test is carried out on the MIKRON UCP710 Five-axis CNC Machining Center, and the actual experimental setup is as shown in Fig. 15. The scheme of the high speed cutting experiment is shown in Table 5.
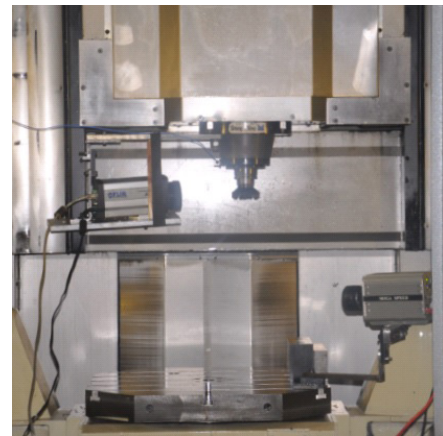

Fig. 15. *Machining field of high speed milling cutter*

Table 5. *High speed milling test schemes*

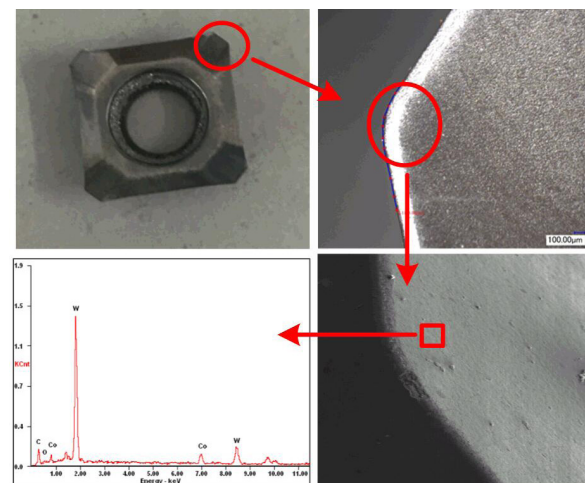| Cutting speed v [m/min]	Milling depth a_p [mm]	Feed per tooth f [mm/r]	Milling width a_e [mm]
2000	0.5	0.08	56
2600	1.0	0.15	56

Fig. 16. *Micro morphology of milling cutter insert*

The test adopts the cutting parameters which are the same as those in simulation. Among them, the insert is WALTER SEHW1204 WKP35, which is the tungsten carbide coating, and the energy spectrums of the insert are as shown in Fig. 16.

4 RESULTS AND DISCUSSION

The simulation test was carried out on two milling cutters with the same structure and components.
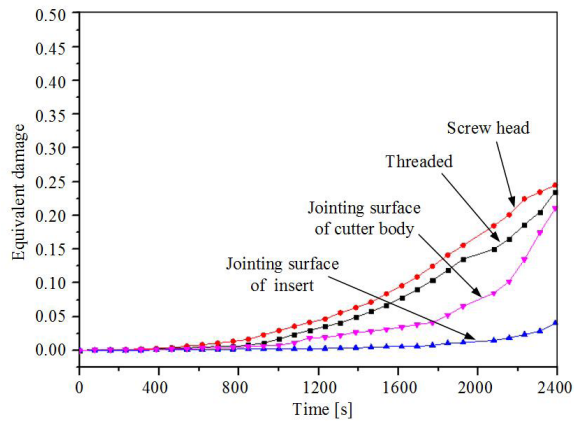

Fig. 17. *Evolution of the milling cutter tooth damage*

The evolution of the cutter tooth damage in the revised program is shown in Fig. 17. The damage degree of the screw and the junction surface of the two milling cutters are obtained through finite element simulation, as shown in Fig. 18.
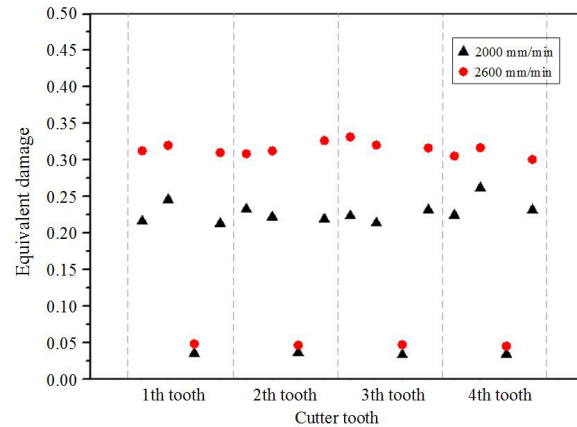

Fig. 18. *Comparison of the damage degree of each cutter tooth under different cutting parameters*

It can be seen from Fig. 18 that the milling cutter suffered from a high degree of damage at larger cutting speed, because the cutter teeth suffer from periodic
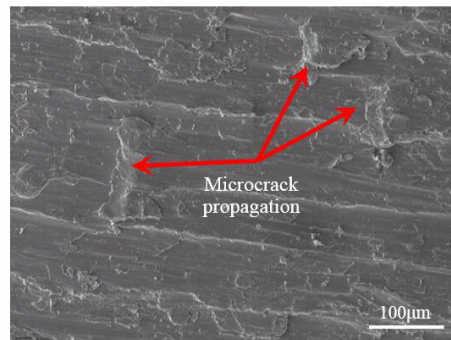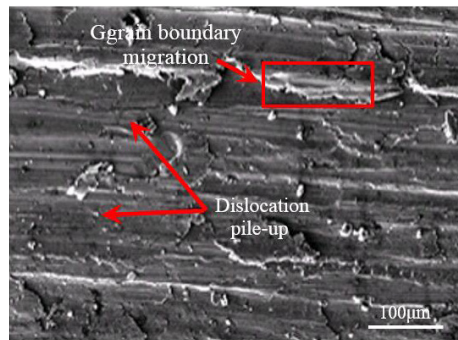

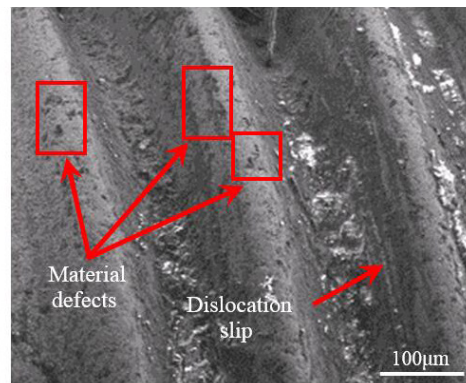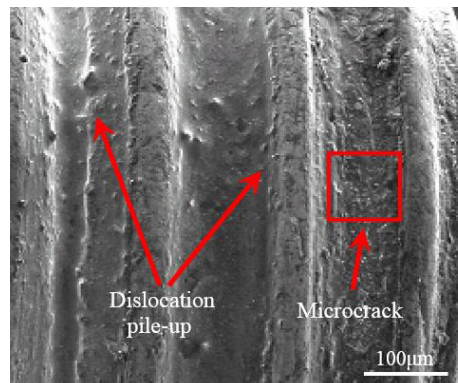**Fig. 19.** *Detection results of the milling cutter joint surface*

Fig. 20. *Detection results of the screw thread*

shocks constantly in the process of cutting, which causes damage to the milling cutter components. In the cutting process, different parts of the teeth suffer from different degrees of damage due to the impact of the cutter vibration, insert installation error and machine tool environment.

After cutting, the damage detection of two milling cutters is carried out, and the results are shown in Figs. 19 and 20.

The grain boundary migration, micro crack propagation and crystal surface cleavage were observed at the joint surface of the tested milling cutter with higher cutting speed by comparing and analyzing the damage detection results of two milling cutters. Obvious damage and small scale structural damage characteristic are shown. In terms of the tested milling cutter with lower cutting speed, there is only a dislocation band in the joint surface of the cutter. Dislocation slip, dislocation pileup and other micro plastic deformation mainly occur in this band, and no obvious damage or structural destruction is found. The result is consistent with that of the milling cutter damage model, which shows that the milling cutter damage evaluation method can be used to judge the damage degree of the milling cutter.

Based on the damage model, simulation and tests results of the high speed milling cutter, the damage formation and evolution process under the condition of cutting load are analyzed. The characteristic curve of the high speed milling cutter damage evolution process is shown in Fig. 21. According to the curve, the process of safety deterioration of the milling cutter caused by the damage can be proved, and the damage state of the milling cutter can be determined.

In Fig. 21, I is the damage characteristic curve of the milling cutter in the safe and stable cutting process. In this process, the injury does not continue to develop, and steady cutting is achieved later. II is the characteristic curve of the slowly developing damage which continues to evolve after occurrence until the critical value is reached. The safety performance of the milling cutter presents dynamic security recession characteristics. III is the damage characteristic curve when the milling tool passes stage I, and the damage reaches the critical value rapidly and develops continuously until the integrity failure occurs. The effect of cutting loads σ_0, σ_1 and σ_2 is mainly affected by the load conditions in the cutting process. δ_0, δ_1, δ_2 and δ_3 depend on the material properties of the milling cutter components and the macro-structure of the milling cutter.

Thus, the mathematical model of the damage characteristic curve of the milling cutter can be constructed, as shown in Eq. (15).

$$S = \begin{cases} \psi(x,\sigma) & (0 \leq \sigma \leq \sigma_0) \\ \omega(y,\sigma) & (\sigma_0 \leq \sigma \leq \sigma_1), \\ \xi(z,\sigma) & (\sigma_1 \leq \sigma \leq \sigma_2) \end{cases} \qquad (15)$$

where $\psi(x)$ is the constant in the constitutive relation of the milling cutter's component materials, and it determines the inherent property of the material. In the safety decline stage, the damage varies with the effect of the cutting load of the milling cutter. $\omega(x)$ is the value of the variable in the damage model. $\xi(x)$ is the critical damage to the milling cutter. As long as the yield strength of the material is reached, the cutter integrity failure occurs.

According to the previous analysis of the milling cutter damage, the damage factors of the milling cutter in the above formula are the material properties and the variables obtained by the test. The adoption of this mathematical model can provide theoretical basis for
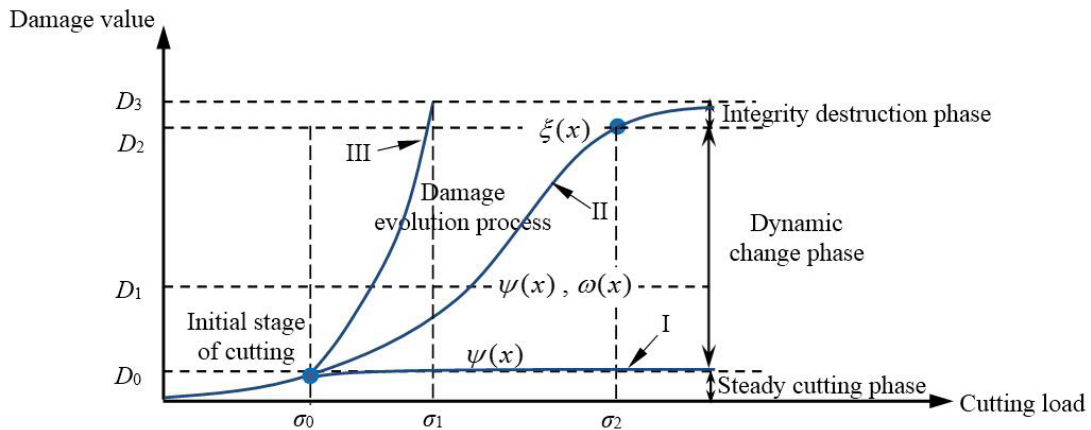

Fig. 21. *Characteristic curve of the damage process of the high speed milling cutter*

analyzing the damage to different parts of the milling cutter.

High speed milling test can be completed using the cutting parameters in Table 3. The unit cutting force is obtained, which is 483.98 N. The initial damage values of the component materials M1 and M2 are found to be 0.0075 and 0.0118, and the critical damage values are found to be 0.1243 and 0.1439, respectively based on the material constitutive relationship of the high speed milling cutter components and the equivalent damage stress value obtained from the compression test.

In order to control the occurrence and development of the damage behavior of the high speed milling cutter, the milling cutter components first meet the ISO 15641 international standard [5]. This requirement is taken to ensure the integrity of the components of the high speed milling cutter in the cutting process as an important prerequisite for the high-speed milling process. This can effectively control the large scale deformation and integrity damage of the milling cutters, but it cannot restrain small scale deformation and damage. Therefore, on the basis of the milling cutter meeting the ISO 15641 standard, the damage evaluation method of the high speed milling cutter is put forward, as shown in Fig. 22.

5 CONCLUSIONS

Under the requirements of high efficiency, high machining quality and high life expectancy for the high speed milling cutter, the decline of the cutting stability and tool life caused by the damage cannot be judged only using existing norms and standards. In this paper, the damage areas of the milling cutter are recognized, and the method of judging the damage of the milling cutter is given. The main research conclusions are as follows:

I. Under the action of the centrifugal force, the instantaneous cutting force and the pre-tightening force, the analyses of the deformation of the milling cutter components demonstrate that damage areas include: the junction surface of the insert and the cutter body, the junction surface of the insert and the screw, the junction surface of the cutter body and the screw and the root of the cutter tooth.

II. The analyses of the damage detection and the test of the mechanical property indicate that, the compression damage, ductility fracture and tensile fracture occur in the joint surfaces of the milling cutter components, due to the dislocation
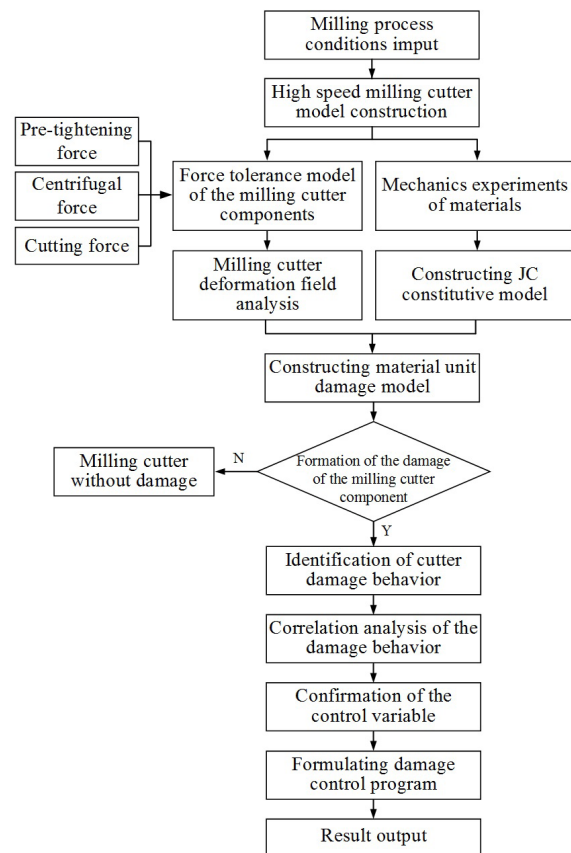

Fig. 22. *Recognition and judgment method of milling cutter damage behavior*

slip, the dislocation pile-up, the grain boundary migration and microcrack propagation generated under the action of the centrifugal force, the pre-tightening force and the cutting force.

III. The component material experiments are conducted to fit the curve of stress-strain and obtain the strain rates in instantaneous and certain action time with high strain rate and without high strain rate. Subsequently, the constitutive relationship is modeled.

IV. A model of the damage evolution of the milling cutter is established based on the equivalent damage, which can reflect the extent of the damage of the milling cutter. Combining with the finite element simulation results, the initial value and critical value of the component damage are obtained to introduce the process of the damage evolution. Finally, experimental results of two cutting test schemes are provided to verify the evaluation method of the milling cutter damage method.

6 ACKNOWLEDGEMENTS

7 REFERENCES

[1] Mativenga, P.T., Hon, K.K.B. (2005). Wear and cutting forces in high-speed machining of H13 using physical vapour deposition coated carbide tools. *Proceedings of the Institution of Mechanical Engineers, Part B: Journal of Engineering Manufacture*, vol. 219, no. 2, p. 191-199, **DOI:10.1243/095440505X8127**.

[2] Tamás, P., Illés, B. (2016). Process improvement trends for manufacturing systems in industry 4.0. *Academic Journal of Manufacturing Engineering*, vol. 14, no. 4, p. 119-125.

[3] Lin, P.T., Gea, H.C., Jaluria, Y. (2011). A modified reliability index approach for reliability-based design optimization. *Journal of Mechanical Design*, vol. 133, no. 4, p. 44-50, **DOI:10.1115/1.4003842**.

[4] Biriş, C. (2016). Considerations on manufacturing accuracy and surface quality of NC laser cutting machine tools. *Academic Journal of Manufacturing Engineering*, vol. 14, no. 2, p. 33-39.

[5] ISO 15641:2001. *Milling Cutters for High Speed Machining - Safety Requirements*. International Organization for Standardization. Geneva.

[6] Beňo, J., Maňková, I., Vrábel, M., Karpuschewski, B., Emmer, T., Schmidt, K. (2012). Operation safety and performance of milling cutters with shank style holders of tool inserts. *Procedia Engineering*, vol. 48, no. 1, p. 15-22, **DOI:10.1016/j.proeng.2012.09.479**.

[7] Ren, H., Li, X.D., Li, J.C. (2010). Numerical simulation and virtual failure of particle reinforced composite microstructure. *Journal of Mechanical Engineering*, vol. 46, no. 4, p. 35-41, **DOI:10.3901/JME.2010.04.035**.

[8] Cheng, M.H., Cao, Y.Z., Peng, H.W., Yang, G.Y. (2015). Influence of microstructural changes on the macro response of functionally graded material structures. *Materials Research Innovations*, vol. 19, no. 8, p. 835-839, **DOI:10.1179/1432891715Z.0000000001815**.

[9] Ge, C.F. (2011). The identification analysis for macro distributions curves of functionally graded materials properties based on materials components. *Advanced Materials Research*, vol. 228-229, p. 50-54, **DOI:10.4028/www.scientific.net/AMR.228-229.50**.

[10] Barabash, R.I., Bei, H., Gao, Y.F., Ice, G.E. (2010). Indentation-induced localized deformation and elastic strain partitioning in composites at submicron length scale. *Acta Materialia*, vol. 58, no. 20, p. 6784-6789, **DOI:10.1016/j.actamat.2010.09.004**.

[11] Birck, G., Iturrioz, I., Lacidogna, G., Carpinteri, A. (2016). Damage process in heterogeneous materials analyzed by a lattice model simulation. *Engineering Failure Analysis*, vol. 70, p. 157-176, **DOI:10.1016/j.engfailanal.2016.08.004**.

[12] Jiang, B., Song, J.G., Wang, S.T. (2012). Model of intrinsic/extrinsic about the safety for high speed milling tools on mesoscale. *Advanced Materials Research*, vol. 500, p. 198-204, **DOI:10.4028/www.scientific.net/AMR.500.198**.

[13] Lorenzini, G., Helbig, D., da Silva, C.C.C., Real, M.V, dos Santos, E.D., Isoldi, L.A., Rocha, L.A.O. (2016). Numerical evaluation of the effect of type and shape of perforations on the buckling of thin steel plates by means of the constructal design method. *International Journal of Heat and Technology*, vol. 34, no. 1, p. 9-20, **DOI:10.18280/ijht.34Sp0102**.

[14] Kruch, S., Chaboche, J.-L. (2011). Multi-scale analysis in elasto-viscoplasticity coupled with damage. *International Journal of Plasticity*, vol. 27, no, 12, p. 2026-2039, **DOI:10.1016/j.ijplas.2011.03.007**.

[15] Burgess, S.C. (2012). A backwards design method for mechanical conceptual design. *Journal of Mechanical Design*, vol. 134, no. 3, p. 213-221, **DOI:10.1115/1.4005620**.

[16] Faassen, R.P.H., van de Wouw, N., Oosterling, J.A.J., Nijmeijer, H. (2003). Prediction of regenerative chatter modeling and analysis of high-speed milling. *International Journal of Machine Tools and Manufacture*, vol. 43, no. 14, p. 1437-1446, **DOI:10.1016/S0890-6955(03)00171-8**.

[17] Qian, S.R., Qin, S.J., Shi, H.S. (2017). Influencing factors of peridynamics analysis and calculation. *International Journal of Heat and Technology*, vol. 35, no. 2, p. 398-402, **DOI:10.18280/ijht.350224**.

[18] Ji, S.Y., Liu, X.L., Ma, D.L., Ding, Y.P., Wu, J. (2011). Parametric design of face milling cutter based on UG template model. *Advanced Materials Research*, vol. 188, p. 336-339, **DOI:10.4028/www.scientific.net/AMR.188.336**.

[19] Horii, H., Nemat-Nasser, S. (1986). Brittle failure in compression: splitting, faulting and brittle-ductile transition. *Philosophical Transactions of the Royal Society of London, Series A: Mathematical and Physical Sciences*, vol. 319. no. 1549, p. 337-374, **DOI:10.1098/rsta.1986.0101**.

[20] Johnson, G.R., Cook, W.H. (1983). A constitutive model and data for metals subjected to large strains, high strain rates and high temperatures. *Proceedings of the 7th International Symposium on Ballistics*, The Hague, p. 541–547.